Proceedings of
11th European Conference on Turbomachinery Fluid dynamics & Thermodynamics
ETC11, March 23-27, 2015, Madrid, Spain

INFLUENCE OF A MULTI-HOLE PRESSURE PROBE ON THE FLOW FIELD IN AXIAL-TURBINES

J. Aschenbruck - T. Hauptmann - J.R. Seume

Institute of Turbomachinery and Fluid Dynamics (TFD), Leibniz Universitaet Hannover,
Hannover, Germany, aschenbruck@tfd.uni-hannover.de

ABSTRACT

To continuously improve jet-engines, it is necessary to precisely predict gas turbine flow fields using computational fluid dynamics (CFD). The results of the simulations are validated with pressure probe measurements. The pressure probe is intended to determine the flow field between the blade rows but as the probe is positioned in the flow passage, it disturbs the flow field.

This study investigates the influence of a multi-hole pressure probe on the flow field in a multistage axial air-turbine. To this end, probe measurements are conducted, and the experimental results are compared to the results of CFD simulations. These simulations are done with and without the probe in the flow passage to investigate the effect the probe has on the flow field numerically.

The simulations with and without probe are in good agreement for flow areas with low gradients. In areas with high velocity gradients, the probe shifts the vane wake circumferentially and reduces the wake magnitude. The numerical probe measurements agree well with the experimental probe measurements especially in the wake region. Based upon these results, the differences between probe measurements and numerical results are mainly caused by the potential effect of the probe. This effect must be considered in the analysis of experimental data of multi-hole pressure probes.

NOMENCLATURE

c	velocity	$m \cdot s^{-1}$	p_{tot}	total pressure	Pa
CFD	Computational Fluid Dynamics		Pr	Prandtl Pitot tube	-
d	probe diameter	m	SPC	static pressure coefficient	-
GCI	Grid Convergence Index		T	static temperature	K
in	value at turbine inlet		TPC	total pressure coefficient	-
$\dot{m}$	mass flow	kg/s	T_{tot}	total temperature	K
Ma	Mach number	-	YAC	yaw angle coefficient	-
MP	measuring plane		y^+	dimensionless wall distance	-
n	rotational speed	rpm	α	yaw angle	°
out	value at turbine outlet		γ	pitch angle	°
p	static pressure	Pa	x,y,z	Cartesian coordinates	
PAC	pitch angle coefficient	-	$1,2,3,4,5$	pressure holes 1,2,3,4,5	

INTRODUCTION

One main excitation mechanism of turbine blades is caused by the wake region of the upstream blade row. In order to measure the wake region, pneumatic multi-hole pressure probes are widely used. Using these probes, the total pressure, static pressure and flow angles can be determined in a rotating machine. In most cases, a thermocouple is supplied so the temperature can also be measured. Different pneumatic probe types can be used to measure the flow field. Rieß and Braun

(2003) recommend a cylindrical probe for measuring in turbomachines due to the good aerodynamic behavior and to minimize the influence on the flow field.

Before a probe can be used, it has to be calibrated in a steady and homogeneous flow field with low turbulence. The calibration coefficients are a function of Mach number and flow angle while Reynolds number effects can be neglected (Bohn et al. 2000, Rieß and Braun 2003, Herbst et al. 2011). These flow conditions at the calibration are not identical to those in turbomachines. The flow field in turbomachines is unsteady and inhomogeneous with high velocity gradients. Additionally, the positioning of the pressure probe between the blade rows leads to a blockage of the flow channel. This blockage effect causes deviating velocities and flow angles at the holes of the probe (Bohn et al. 2000, Humm 1996, Herbst et al. 2011). Besides the blockage effect of the probe, unsteady and high velocity gradients have a significant influence on the accuracy of pneumatic probe measurements. The interaction between probe, flow, and blades due to the small axial gap has to be considered in the measurements. This can be directly influenced by the probe's design and the measurement setup (Bohn et al. 2000, Herbst et al. 2011, Hoenen et al. 2012).

Numerical investigations of the influence of pneumatic pressure probes on the flow field and the measurement accuracy were conducted in previous studies (Seume et al. 2006, Coldrick et al. 2004a, Coldrick et al. 2004b, Herbst et al. 2011). Coldrick et al. (2004a) investigated the influence of probe measurements between a rotor blade row and a stator vane row in an axial compressor. The main objective of this research was the comparison of the numerical results with and without probe. The main result was that the unsteady flow in a compressor has little influence on the characteristics of the probe. In Seume et al. (2006) the unsteady interactions between a four-hole probe, the flow, and the blades of an axial compressor were numerically investigated, and the results were validated with experimental data. It was shown that a numerical calibration of the aerodynamic probe is necessary for these numerical investigations. Such a numerical calibration for a four-hole cobra-probe is presented in Herbst et al. (2011) using a model of typical free-jet calibration channel. The calibration is used in a numerical investigation of the probe's influence in an axial turbine. The results of the numerical calibration agree well with the experimental calibration data for small flow angles. However, the results of the numerical measurements in the turbine show significant differences with and without probe, due to potential effects on flow areas with high velocity gradients. A correction method for measurements with a five-hole probe in gradient wake flows is presented in Hoenen et al. (2012). This correction was set up by measuring a compressor profile in a free stream. The wake flow was measured with different measurement techniques. The measurement error can be reduced by the correction method in flow areas with high gradients.

An accurate prediction of the flow field between stator and rotor blade rows is necessary, especially of the magnitude of the vanes wake to determine the excitation of the downstream blade rows. In literature (Sans et al. 2013, Herbst et al. 2013, Aschenbruck and Seume 2013) an overestimation of the vane wake by CFD compared to probe measurements was observed. The main objective of this paper is to investigate the influence of a five-hole pressure probe on the flow field between the blade rows in the five stage axial turbine of the Institute of Turbomachinery and Fluid Dynamics. For this investigation, a numerical and experimental calibration of the probe is conducted and the results are compared. In the next step, the last stage of the axial turbine is simulated using CFD with and without the probe to determine the influence of the probe. Finally, the numerical "measurements" are compared with the experimental results from the turbine tests to extract the uncertainties caused by the CFD simulations. The analysis of the flow parameters from the simulations with the probe is carried out identically to the experimental analysis.

FIVE-HOLE PRESSURE PROBE

In this study a five-hole cylindrical pressure probe with hemispherical head is used to determine the flow field between the stator and rotor blade rows in axial turbines. This probe type is often used for measurements in turbomachines with high velocity gradients because of the good dynamic behavior as described in Rieß and Braun (2003). However, measurement errors due to flow

gradients in the turbine can still occur. This probe type is not applicable in near-wall regions because of its specific geometry shape, i.e. the thermocouple prevents measurements close to the hub (Fig.1). Accurate results can be achieved with this probe type in an inhomogeneous flow field. The probe head has a diameter of 5 mm and features five small holes as illustrated schematically in Fig. 1. Each of these five tubes has a diameter of 0.5 mm and measures the pressure. Normally the probe is almost aligned with the flow direction such that hole 1 in the center of the probe head measures the total pressure. The other four holes are distributed symmetrically around hole 1. The holes 2 and 3 are used to determine the yaw angle α and the holes 4 and 5 to measure the pitch angle γ. The definition of the yaw and pitch angle α and γ is shown in Fig. 1.

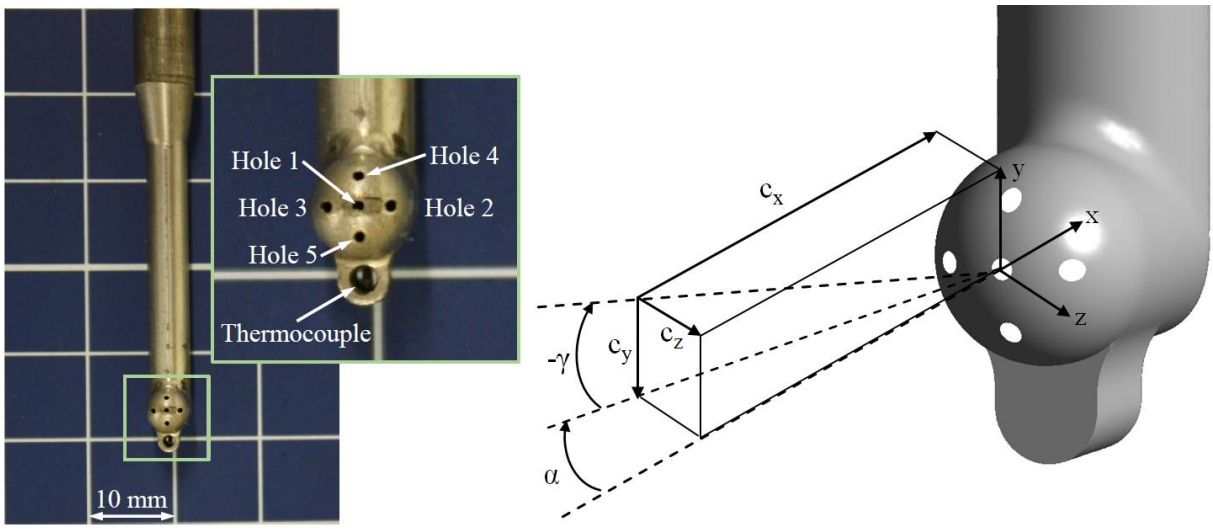

Figure 1: Five-Hole pneumatic probe numeration (Aschenbruck and Seume 2014) (left) and definition of yaw angle α and pitch angle γ in accordance to Rieß and Braun (2003) (right)

The total pressure and static pressure can be determined by analyzing these five pressure values. For this analysis a calibration of the probe is necessary, which is presented in the following section. In addition to the total pressure, static pressure, and flow angles, it is also possible to capture the temperature with the thermocouple below the hemispherical probe head. Using this additional information it is then possible to determine the velocity and the Mach number.

CALIBRATION OF THE AERODYNAMIC PROBE

The flow field in axial turbines between rotor and stator is unsteady with high flow gradients. The measurement of this flow field using an aerodynamic probe is complicated due to the probe influences on the flow field. Thus, the measured pressures in pressure holes are not equal to the pressure in the undisturbed flow field. For this reason, the pressure probe has to be calibrated in a steady and homogenous flow field to correlate the measured values to the values of an undisturbed, known flow field. This calibration is carried out in a high-speed-calibration channel. The complete calibration method is described in the following section and is similar to the calibration described in Herbst et al. (2011) and Rieß (2003).

Calibration Method and Data Analysis

The calibration of aerodynamic probes consists of several steps. In the first step, measurements are conducted with the probe in a calibration duct with a known, steady and homogenous flow field. The pressures at the pressure holes are determined for different Mach numbers at varied pitch and yaw angles (α and γ). This is done by rotating and tilting the probe around pressure hole 1.

After the pressures are measured in the calibration duct, the calibration coefficients are determined as a function of Mach number and flow angles α and γ. These coefficients are defined as yaw angle coefficient

$$YAC = \frac{p_2 - p_3}{p_1 - (\mathrm{p}_2 + \mathrm{p}_3 + \mathrm{p}_4 + \mathrm{p}_5)/4} \tag{1}$$

for the yaw angle α, pitch angle coefficient

$$PAC = \frac{p_4 - p_5}{p_1 - (\mathrm{p}_2 + \mathrm{p}_3 + \mathrm{p}_4 + \mathrm{p}_5)/4} \tag{2}$$

for the pitch angle γ, total pressure coefficient

$$TPC = \frac{p_{t,Pr} - p_1}{p_1 - (\mathrm{p}_2 + \mathrm{p}_3 + \mathrm{p}_4 + \mathrm{p}_5)/4} \tag{3}$$

for the total pressure p_t and static pressure coefficient

$$SPC = \frac{p_{Pr} - (\mathrm{p}_2 + \mathrm{p}_3 + \mathrm{p}_4 + \mathrm{p}_5)/4}{p_1 - (\mathrm{p}_2 + \mathrm{p}_3 + \mathrm{p}_4 + \mathrm{p}_5)/4} \tag{4}$$

for the static pressure p.

In the next step, these calibration coefficients are used to analyse the measurement data. The analysis is an iterative process, as the flow angles depend on the Mach number. For this reason the Mach number must be estimated in the first iteration to determine the flow angles α and γ using the *YAC* and *PAC*. From this the *TPC* and *SPC*, which are dependent on the flow angles and Mach number, can be determined from the calibration data. The total and static pressure can then be calculated using the *TPC* and *SPC*. After this step the next iteration starts with a new calculation of the Mach number using the total and static pressure and all the following steps. This iteration loop stops when the difference between the Mach number of the last iteration and the iteration before is less than $1 \cdot 10^{-6}$. This analysis of the measurement data is automatically calculated using a program.

Experimental Calibration

The experimental calibration of the aerodynamic probes takes place in the high-speed-calibration channel of the TFD (see Fig. 2). This channel is operated in an open loop. The maximum Mach number possible is Ma = 1. More information about this channel is presented in Bammert et al. (1973). For the calibration, the probe was positioned one nozzle diameter downstream of the convergent nozzle outlet. The first hole of the probe was positioned at the center line of the free jet for all calibration positions. The experimental calibration was conducted for a yaw angle range of $-12° \leq \alpha \leq 12°$ in 3° steps and for the pitch angle of $-15° \leq \gamma \leq 15°$ in 3° steps. These positions were then calibrated for Mach numbers between 0.1 and 0.6 in 0.1 steps. The total pressure $p_{t,Pr}$ and static pressure p_{Pr} for the total and static pressure coefficients were measured with a Prandtl Pitot tube at the probe's axial location for reference values.

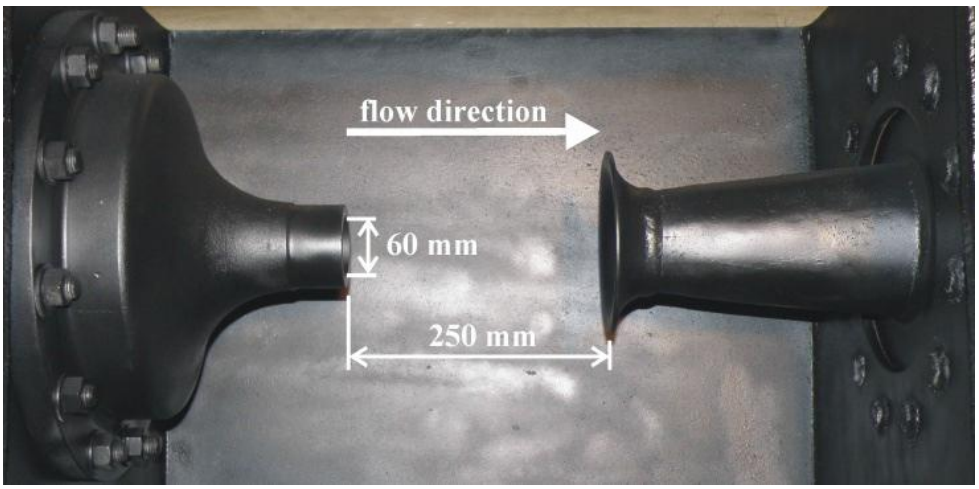

Figure 2: Free jet region of the calibration duct (Herbst et al. 2011)

Numerical Calibration

In accordance with Herbst et al. (2011) the numerical calibration was performed with a model of the high-speed-calibration channel, see Fig. 3. The model of the calibration channel was simplified by modeling only the nozzle and replacing the bellmouth with a volume defined as a boundary with ambient static pressure. Besides the calibration channel, the five-hole pressure probe was also simplified, by covering the pressure holes, the pressure tubes, and the thermocouple with a wall. Nevertheless, the probe was modeled with its characteristic shape, to ensure negligible modeling error between simulations and experiments. The modification of the pressure probe reduces the computational effort in the mesh generation, however the geometry is still complex, thus the probe mesh must be generated with an unstructured mesh around the probe head. The unstructured mesh consists of tetrahedrons and prism-layers close to the wall. The other components of the calibration channel were discretized with structured meshes using hexahedral elements. The meshes for the numerical calibration have a grid quality with a minimum angle of 26° and a maximum aspect ratio below 1700. The total number of grid points is approximately 1.15 million.

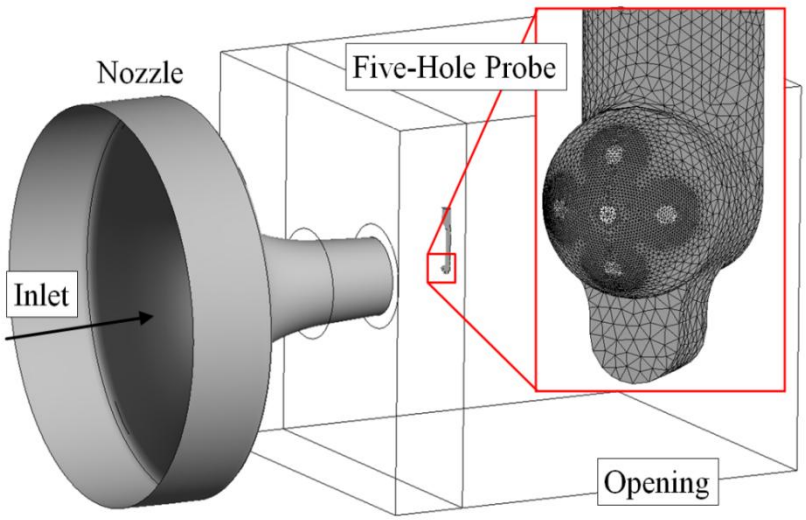

Figure 3: Numerical model of the high-velocity calibration channel with the five-hole pressure probe (in accordance with Herbst et al. 2011)

The boundary condition of the nozzle inlet was set to a constant total pressure corresponding to the specific Mach number. The numerical calibration is performed for two Mach numbers Ma = 0.2 and Ma = 0.4 with varied yaw and pitch angles. These Mach numbers were selected because these

are the relevant values in the last stage of the axial turbine for the investigated operating point. The outflow of the nozzle is homogenous and undisturbed. The probe is located in the middle axis of the free jet. The yaw angle was varied in a range between $0° \leq \alpha \leq 15°$ in 5° steps. The negative yaw angles are neglected because of the symmetrical geometry of the probe. The pitch angle was calibrated for a range $-5° \leq \gamma \leq 5°$ in 5° steps. This pitch- and yaw-angle range should be sufficient to capture the occurring flow angles in the turbine. The simulations of the calibration are done with the CFD-Software ANSYS CFX 14.5 using the SST turbulence model and the high-resolution advection scheme. The SST turbulence model is a combination of the k-ε and k-ω turbulence model and is recommended for high accuracy boundary layer simulations. This model was preferred for the numerical calibration and the calculations in turbine stage because especially the boundary layer and the wakes of stator vanes in the simulation of the turbine are important regarding the accuracy of the simulations and the results of the probe. For the calibration steady simulations are performed with a physical timestep of 0.001s. All simulations reached RMS-Residuals below 10^{-4}, MAX-Residuals below $5 \cdot 10^{-2}$, and mass imbalance below 0.001%. The high maximum residuals are at the sharp edges of the thermocouple mounting below the pressure holes. The sharp edges induce unsteady effects which results in high residuals. Nevertheless, these unsteady effects do not influence the relevant flow near the pressure holes. The results of the numerical calibration can be used because of the stable flow at the pressure holes.

Numerical and Experimental Results

In Figure 4 the numerical and experimental results of the calibration are plotted for the case of *Ma* = 0.2. This Mach number shows similar results when compared to higher velocities. The error bars of the experimental indicate the 95% confidence interval. The *YAC* has a linear characteristic depending on the yaw angle in the range of $-15° \leq \alpha \leq 15°$ and is in good agreement between numerical and experimental results. In Figure 4 it is also pointed out that the *TPC* shows a good accordance of the numerical and experimental calibration data and differs only slightly. However, the diagram of the *TPC* coefficient shows a higher deviation at a yaw angle of $\alpha = 12{,}5°$. This difference is not in the 95% confidence interval. Linear behavior is also visible in the results of the *PAC* calibration coefficient subjected to the pitch angle. Both the numerical and experimental results show linearity but differ by a constant offset. The results of the numerical calibration of the *SPC* coefficient are not in accordance with the experimental results and show differences in dependence on the pitch angle.

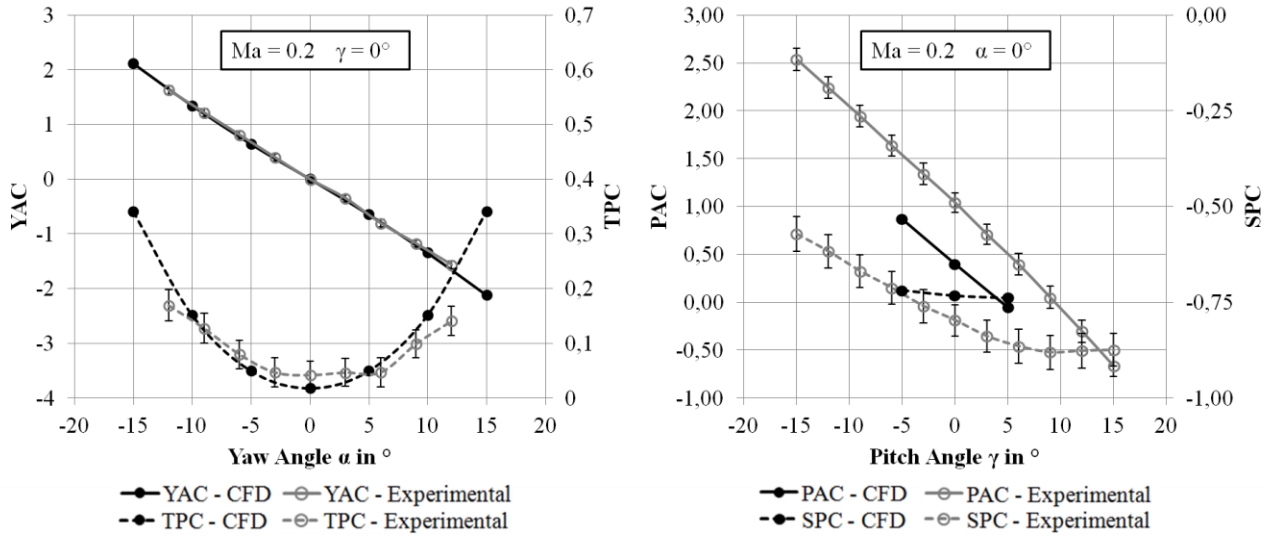

Figure 4: Numerical and experimental calibration coefficients for Ma = 0.2

For high incidences the numerical results are unreliable because flow separation cannot be reproduced accurately by the CFD simulations. The reason for the offset at the *PAC* and the differences at the *SPC* between numerical and experimental results cannot be determined currently. It may result from a modeling error between the simplified model and the real probes geometry. Nevertheless, the comparison shows a good agreement between the calibration coefficients YAC and TPC and will be used below to further investigate the air turbine.

TEST FACILITY

The numerical and experimental investigations were performed in an axial air turbine. The turbine can be equipped with several blade configurations for investigations of efficiency, aerodynamic losses, secondary flows, and aeroelastic effects. For the current study, a five-stage configuration was used, as depicted in Fig. 5. Each stage consists of 29 stator vanes and 30 rotor blades. The rotor blades are mounted in axial fir-tree grooves on the single solid rotor and the vanes in inner casing rings. The fifth stage has been designed with aeroelastic investigations in mind. Further information about this configuration and the design process are given by Aschenbruck et al. (2013).

In this study a part-load operating point is examined in the numerical investigation as well as in the experimental measurements. The parameters of this operating point are given in Tab. 1**.** This study focuses on the measuring plane (MP), which is located between the fifth stator vane row and the fifth rotor blade row (see Fig. 5)**.** This MP is selected to measure the wake of the fifth-stage vane with the five-hole pressure probe. The numerical and experimental results are compared at mid span of the MP. The probe is circumferentially traversed along one pitch downstream of the fifth stator vane.

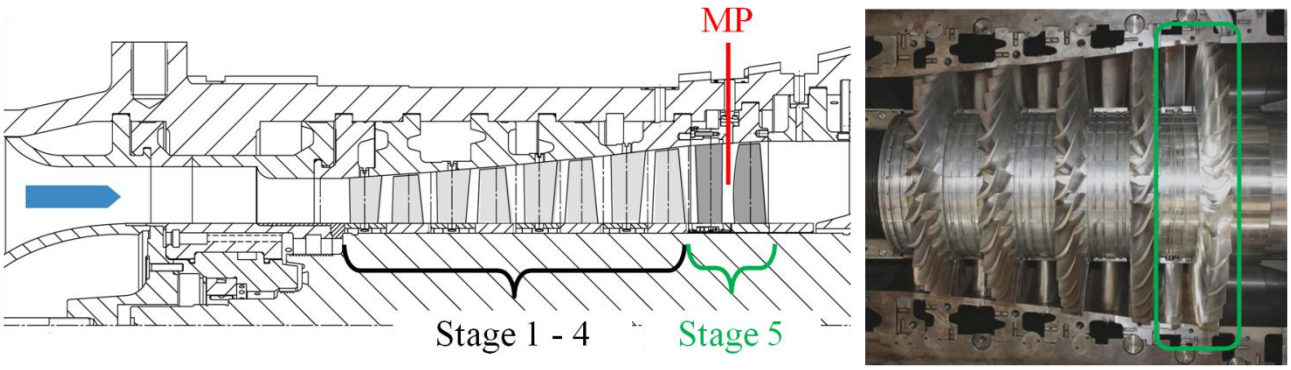

Figure 5: Five-stage air turbine

Table 1: Parameters of the five-stage turbine at part-loaded operating conditions

Mass flow rate $\dot{m}$ in kg/s	Rotor speed n in rpm	Pressure ratio p_{in}/p_{out}	Inlet Temperature T_{in} in K	Outlet Temperature T_{out} in K	Mach number in MP Ma
4,3	4000	1,58	364	324	0,31

NUMERICAL PROBE MEASUREMENTS IN THE TURBINE

Numerical Setup

The investigations of the flow field with and without the five-hole pressure probe were conducted in the fifth stage of the axial turbine between the stator vanes and rotor blades. The numerical setup of the steady simulations is depicted in Fig. 6. A constant mass flow rate and total temperature were set at the inlet and an average static pressure was assumed at diffuser outlet,

according to the operating point in the experiments. In the steady simulations, the interface between stator vane mesh and the probe mesh was defined as a frozen rotor interface. This interface was selected to make sure that the wake behavior is propagated into the probe domain. The interfaces between the probe domain and rotor blade domain as well as between the rotor and diffuser domain were defined as mixing planes. Instead of 29 vanes and 30 blades, the stator vane row and the rotor blade row were modeled with 30 airfoils to ensure an equal pitch of the domains. The simulations used a 60° segment and rotational periodicity is defined at the circumferential boundaries. In this segment, five vanes, five blades and one probe were modeled. Due to the rotational boundary conditions, the setup is equal to a measurement with six probes which are equally spaced on the circumference. The blockage caused by the probes was investigated by Herbst et al. (2011) for a similar model. They have shown that the influence on the performance of the whole turbine is negligible.

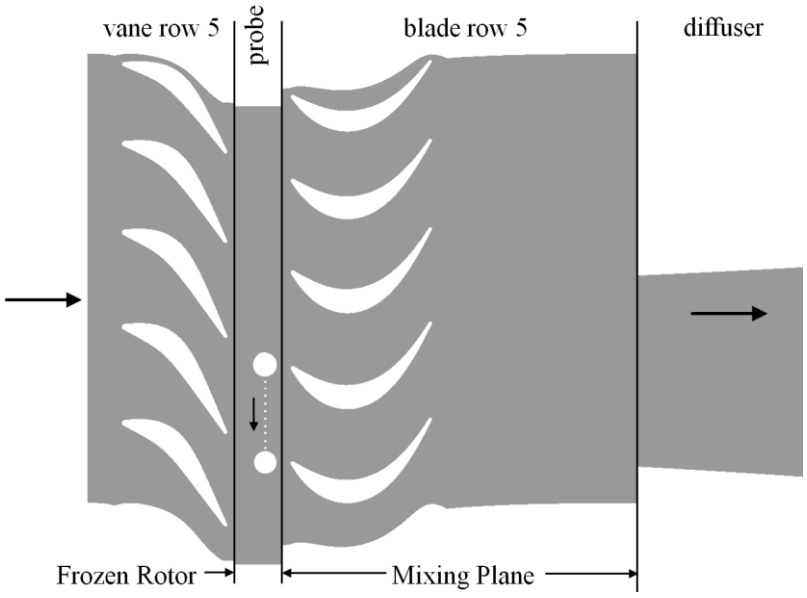

Figure 6: Numerical Setup of steady simulations with probe (probe traversed locations indicated)

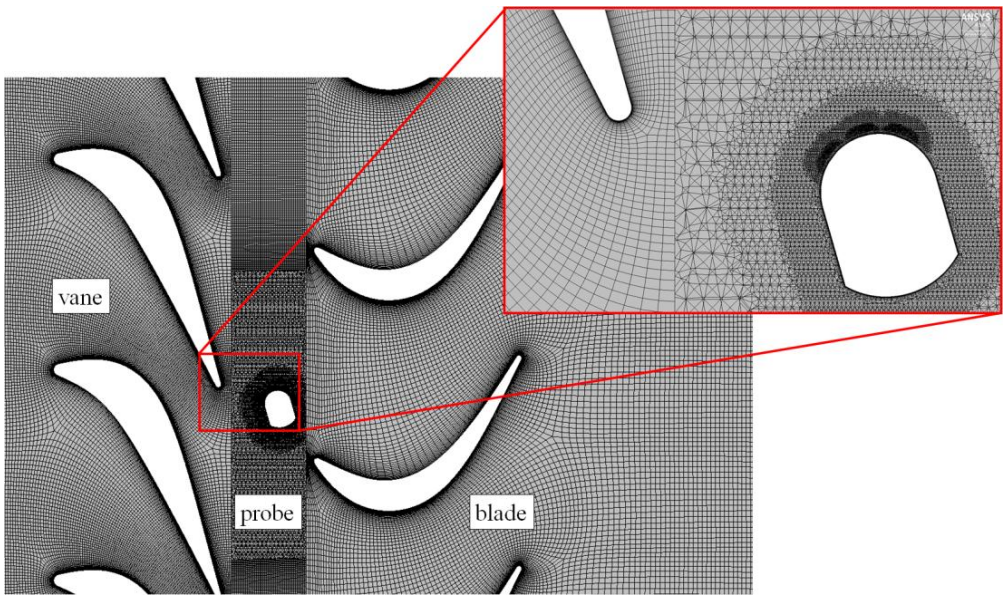

Figure 7: Mesh Resolution of the fifth stage at mid span

The stator, rotor, and diffuser domain was meshed solely with hexahedral elements. The domain with and, for consistency, without a probe was meshed with a hybrid mesh (see Fig. 7). The middle part of the hybrid mesh was discretized with an unstructured mesh around the probe using tetrahedrons and prisms in the near wall-region. The left and right part of the hybrid mesh was a structured mesh with hexahedral elements. The meshes for the numerical calculation of the turbine stage have a grid quality with a minimum angle of 30° and a maximum aspect ratio below 1700. The cell distance and cell growth in all meshes is similar to ensure that the wake is not mixed out at the interfaces between the stator and probe domain. The complete numerical model including the probe consists of about 9.36 million nodes and without the probe around 9.23 million nodes. The hybrid mesh of the probe domain with the probe has around 3 million nodes. This high resolution is necessary to minimize the discretization errors and to obtain accurate pressure values at the probe location.

For the numerical investigations, it is important that the numerical error caused by the mesh resolution is negligible. For this purpose, a mesh study of the hybrid mesh was performed on the most relevant parameters of the study and was evaluated by the Grid Convergence Index (Salas, 2006). These are the pressure values at the holes of the probe. Table 2 presents the results of the mesh study for the pressures at probe hole 1. The pressure is almost independent of the mesh resolution. The fine mesh was used for the following investigations in order to capture the correct flow field in exchange for greater computational effort. The stator, rotor and diffuser meshes were analyzed in a previous study and have a sufficient mesh resolution.

Table 2: Results of mesh study for the hybrid mesh

Mesh	*Nodes*	*Grid convergence index for pressure at probe hole 1*
Coarse (grid 3)	1.554.504	0,0061
Medium (grid 2)	2.463.440	0,0038
Fine (grid 1)	3.086.877	0,0030

The probe was positioned at 50% channel height. For the numerical "measurements" the probe was rotated 74° counterclockwise in order to avoid high yaw angle incidence. The probe was traversed circumferentially about one pitch (12° segment) in 1° steps to measure the flow field of one pitch. The increment of 1° is sufficient to capture the regions with high velocity gradients like the wake region. The flow field without a probe was determined at mid span and at the same axial position where the pressure hole 1 of the probe would be located. Similar to the numerical calibration, the simulations were performed with ANSYS CFX 14.5 using the SST turbulence model and the high-resolution advection scheme. All simulations reached RMS-Residuals below $3 \cdot 10^{-4}$, MAX Residuals below $5 \cdot 10^{-2}$, and mass imbalance below 0.01%. The highest residuals are located in the wake region of the probe. The flow near the holes of the probe is not influenced by this wake and shows good convergence behavior.

Numerical Results

The results of the simulation without probe are compared with the simulations with probe in order to determine the influence of the probe on the local flow field. For this comparison, steady simulations were conducted and analyzed. In Figure 8 (left) the normalized total pressure $p_{tot}/p_{tot,in}$ is shown as a function of the pitch for one vane passage. The total pressure at turbine inlet $p_{tot,in}$ was previously determined by steady CFD simulation of the 5 stage turbine (for more information see Aschenbruck et al., 2013). A good agreement of the total pressure between the steady simulations with and without probe is visible in the region with low flow gradients from 0 to 40% of the pitch. This good agreement is because the probe is calibrated in a flow field with low flow gradients. A shift of the wake occurs in the simulation with probe compared to the simulation without probe. The position of the wake shifts in the circumferential direction by 5% pitch and the magnitude of the deficit in total pressure is reduced by 0.15%.

These differences occur due to the interaction of the probe with the blades and the fluid. To illustrate this effect, the total pressure distribution is depicted at mid span for different probe positions and for the simulation without the probe in Fig. 9. The probe positions are marked in the pressure distribution of the simulation without probe. The numerically determined total pressure at the 7° probe position is higher compared to total pressure in the simulations without probe. This is due to the displacement effect of the probe on the wake at this position, shifting the wake in the circumferential direction (see Fig. 9 a) whereas the total pressure in the simulation without the probe is not influenced by the wake at this position. At the 9° position of the probe, the wake is still shifted in the same circumferential direction. Hence, the probe is almost in the middle of the wake, and has a lower total pressure compared to the total pressure of the simulation without probe. The total pressure is not as low as the minimum total pressure in the middle of the vane wake in the simulation without the probe (11° position). This reduction of the magnitude of the deficit in the total pressure is caused by a higher mixing of the gradients due to the upstream-acting potential effect of the pressure probe.

At the 11° position of the probe, the numerically determined total pressure is higher compared to the results without the probe. The vane wake is now shifted in the other circumferential direction due to the potential effect between the blade's suction side and the probe, whereas the undisturbed vane wake has its minimum at this position (see Fig. 9 d).

The results of the Mach number (see Fig. 8, right) show similar differences in the wake prediction as was detected for the normalized total pressure. The position of the wake is also shifted in the circumferential direction by 5% pitch for the same reasons as described above. In contrast to the total pressure, the magnitude of the deficit in the Mach number is higher for the numerical probe "measurements". The Mach number over the whole pitch is lower compared to the results of the simulations without the probe. This difference is caused by a lower outlet flow angle of the stator vanes, which is shown in Fig. 11, and thus the Mach number is reduced. In Fig. 11 the yaw angle α is shown as a function of the pitch for one vane passage. The angle is approximately 1° lower between 15% and 60% pitch in the case with probe. In the wake region this differences increases up to 3°. This change in the flow angle is caused by the displacement and potential effect of the probe head which is in accordance to the results presented in Fig. 8.

The disturbance of the probe on the flow field is visualized in Fig. 10 for the 9° position of the probe. The Mach number is shown as a function of the pitch for three vane passages analyzed 2 mm upstream of the probe head. The influence on the flow is locally limited to two pitches next to the probe. In this probe position, the displacement effect of the probe leads to a deceleration of the flow until the wake. Then the flow is deflected and extremely accelerated. It is visible that the probe is not "measuring" the undisturbed flow because of its own influence on the flow field.

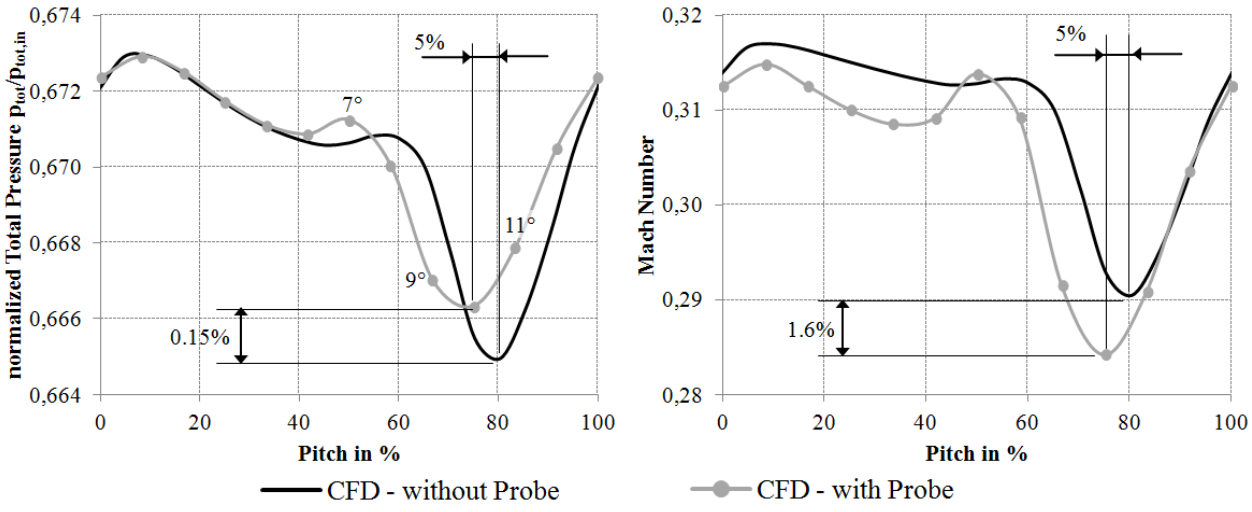

Figure 8: Comparison of flow behavior of numerical results with and without probe

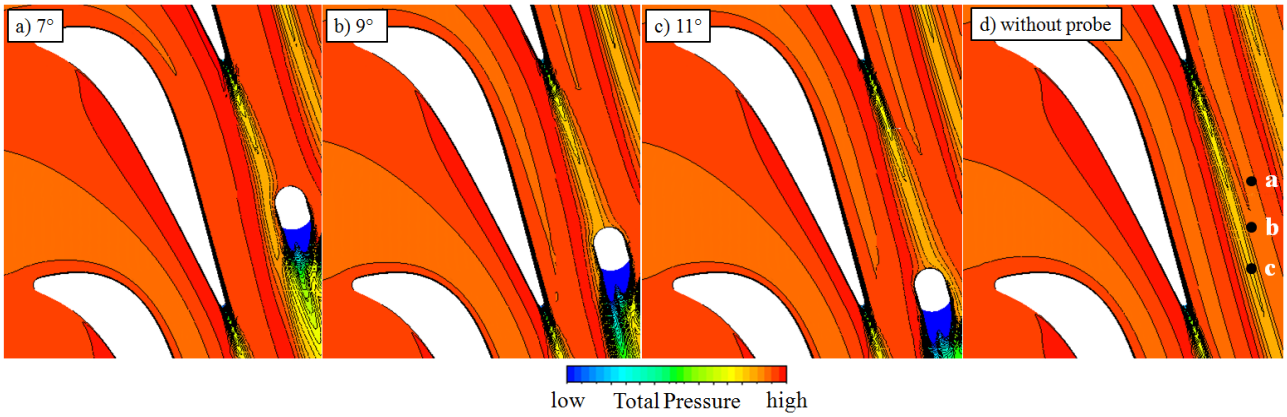

Figure 9: Comparison of the flow field at mid span for different probe positions

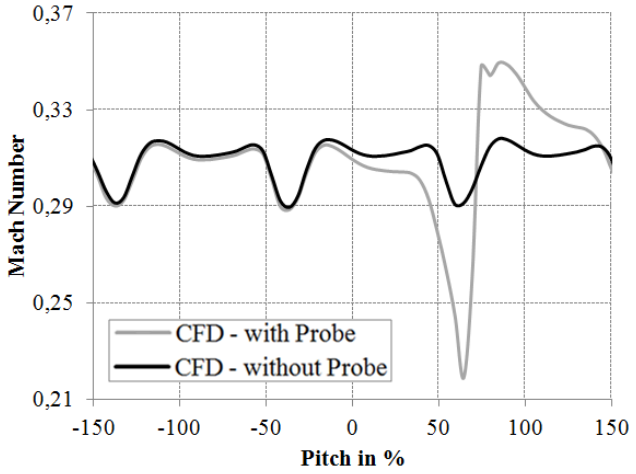

Figure 10: Comparison of Mach number 2 mm upstream of the probe (9° position of the probe)

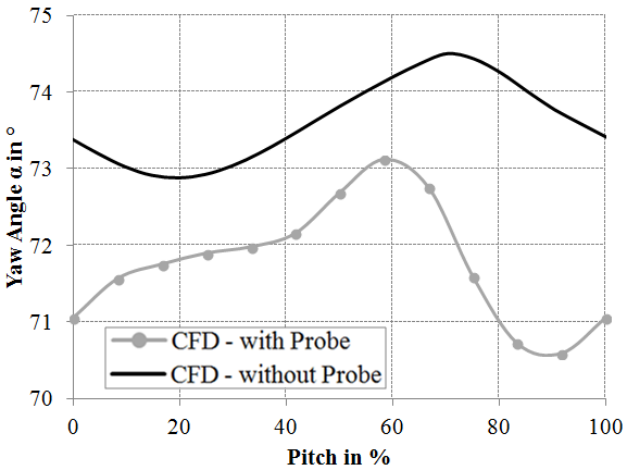

Figure 11: Comparison of the yaw angle α of numerical results with and without probe

EXPERIMENTAL VALIDATION

In order to verify the numerical results, the simulations with the probe were compared with the experimental data of the probe measurement in the turbine. The normalized total pressure and Mach number is plotted in Fig. 12. The experimental results agree well with the numerical results with the probe in the area of 50 to 90% of the pitch. In this area the wake region is predicted accurately by the CFD. The differences are in the 95% confidence intervals which are indicated by the error bars.

However there is a disagreement between the numerical and experimental results in the flow region with low total pressure gradients, between 0 to 50% pitch. The relative total pressure and the Mach number of the simulations are higher compared to the experimental results between 0 and 20% pitch. This difference could be caused by two effects: The values of the measurements at 0 and 100% must be identical as it is a periodic signal. This is not the case for the experimental results (see Fig. 12). Hence, this difference between the values at 0 and 100% might be caused by errors in at the measurements due to positioning tolerances of the probe or due to a drift of the operating point. The second error source is caused by the CFD simulations. The overshoots at 8 and 50% pitch next to the wake region typically occur in CFD simulations. This phenomenon is described by Issa (1994) and occurs in highly turbulent flow, when frictional effects are expected to substantially reduce total pressure. Another error source can be the stage 4 vane wakes which are neglected in the CFD simulations because only the fifth stage was modeled. However, the comparison between the numerical and experimental probe measurements agrees very well for the regions with high pressure gradients.

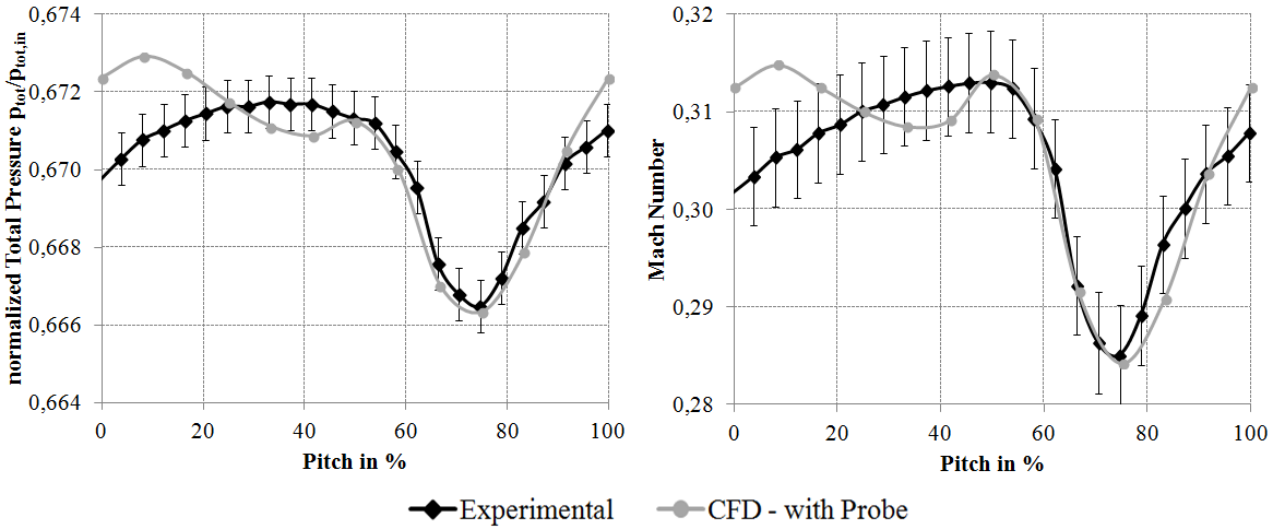

Figure 12: Comparison of experimental and numerical results

CONCLUSIONS and OUTLOOK

The effects of a multi-hole pressure probe on the flow field have been numerically and experimentally investigated. For this purpose the pressure probe was calibrated experimentally and numerically in a high velocity-calibration channel. The comparison of this calibration data shows a good agreement for the calibration coefficients YAC and TPC, which confirms the validity of this calibration procedure for CFD simulations even if differences occur for the calibration coefficients PAC and SPC.

The numerical calibration data were used for the numerical probe measurements in the air turbine conducted by CFD simulations. For these "measurements", the probe was inserted at different circumferential positions in the last turbine stage between the stator vane and the rotor blade row. The results of these simulations were compared with the results of the simulation without the probe. Using this comparison, the influence of the probe on the measured values was determined. It was shown, that differences occur compared to the simulations without the probe in regions with high flow gradients. These differences were caused by the potential effect of the probe and by the interaction between the probe and the stator vanes.

In the last step, a comparison between the experimental and numerical probe measurements was conducted to separate the errors caused by the CFD simulations. This comparison shows a good agreement in the regions with high flow gradients. Thus, the differences between CFD simulations and probe measurements are mainly caused by the influence of the probe on the flow field.

To further improve the probe measurements, the potential effect of the probe should be corrected in the analysis of the measurement data. For this purpose, the probe has to be calibrated in a flow field with typical gradients for turbomachines. This calibration can be done numerically or experimentally and could then be integrated into the standard calibration procedure.

ACKNOWLEDGEMENTS

The authors kindly thank the German Research Foundation (DFG) for the financial support to accomplish the research project C4 "Regeneration-induced Variance of Aeroelastic Properties of Turbine Blades" within the Collaborative Research Center (SFB) 871. Furthermore the authors want to thank Sebastian Keich for his contribution made with the numerical calibration.

References

Aschenbruck, J.; Seume, J.R. (2015): Experimentally verified study of Regeneration-Induced Forced Response in Axial Turbines. Journal of Turbomachinery, March 2015, Vol. 137, Issue 3, 031006 (10 pages), DOI: 10.1115/1.4028350

Aschenbruck, J.; Meinzer, C.; Pohle, L.; Panning-von Scheidt, L.; Seume, J.R. (2013): Regeneration-induced Forced Response in Axial Turbines. Proceedings of the ASME Turbo Expo, June 3-7, 2013, Düsseldorf, Germany, GT2013-95431

Bammert, K.; Bohnenkamp, W.; Woelk, G.-U. (1973): Strömungskanäle zum Kalibrieren von Druck-, Temperatur- und Geschwindigkeitssonden. Konstruktion 25, Vol. 1973, pp. 245-254

Bohn, D.; Funke, H.; Heuer, T. (2000): Sonden-Schaufel-Interaktion bei stationären Messungen mit pneumatischen Strömungssonden in engen Axialspalten. FVV Final Report, Vol. 688-2.

Coldrick, S.; Ivey, P.C.; Wells, R.G. (2004a): The Influence of Compressor Aerodynamics on Pressure Probes – Part 1: In Rig Calibrations. Proceedings of the ASME Turbo Expo, 14-17 June 2004, Vienna, Austria, GT2004-53240

Coldrick, S.; Ivey, P.C.; Wells, R.G. (2004b): The Influence of Compressor Aerodynamics on Pressure Probes – Part 2: Numerical models. Proceedings ASME Turbo Expo, 14-17 June 2004, Vienna, Austria, GT2004-53241

Herbst, F.; Bluemel, S.; Fakiolas, E.; Seume J.R. (2011): Numerical Investigation of the interaction between Probe, Flow and Blading in an Axial-Turbine. 10th International Gas Turbine Congress, 13-18 November 2011, Osaka, Japan, IGTC2011-0194

Hoenen, H.T.; Kunte, R.; Waniczek, P.; Jeschke, P. (2012): Measuring failures and correction mehtods for pneumatic multi-hole probes. Proceedings of the ASME Turbo Expo, 11-15 June 2012, Copenhagen, Denmark, GT2012-68113

Humm, H.J. (1996): Optimierung der Sondengestalt für aerodynamische Messungen in hochgradig fluktuierenden Strömungen. Ph.D Thesis, Eidgenössische Technische Hochschule Zürich, Switzerland

Issa, R.I. (1994): Rise of Total Pressure in Frictional Flow. AIAA Journal, Vol. 33, No. 4: Technical Notes

Rieß, W.; Braun, M. (2003): Stationäres und instationäres Verhalten verschiedener Typen von Strömungsmesssonden in instationärer Strömung. DFG Final Report, Ri 375/13-1, Institute of Turbomachinery and Fluid Dynamics, Leibniz University Hannover, Germany

Salas, M. D. (2006): Some Observations on Grid Convergence. NASA Langley Research Center, Hampton, VA 23681-2199

Sans, J.; Desset, J.; Dell'Era, G.; Brouckaert, J.-F. (2013): Performance testing of a low pressure compressor. Proceedings of the 10th European Turbomachinery Conference, 11-15 April, Lappeeranta, Finland

Seume, J.R.; Herbst, F.; Missirlis, D.; Yakinthos, K.; Goulas, A. (2006): Numerical model of the unsteady interaction between probe and flow in axial turbomachinery. Proceedings XVIII Symposium on Measuring Techniques in Turbomachinery Transonic and Supersonic Flow in Cascades and Turbomachines, 21-22 September 2006, Thessaloniki, Greece